Research paper

Synergy of remote sensing data collected with low-cost mobile mapping platform for detection and prediction of damages: a park alley case study

Magdalena Pilarska-Mazurek[1], Krzysztof Bakuła[2], Jakub Górka[3], Paweł Czernic[4], Anna Lejzerowicz[5], Wojciech Ostrowski[6], Borys Chetverikov[7]

Abstract: Data synergy involves acquiring and combining data from different sensors to achieve better problem analysis and research results. For more comprehensive data analysis, the sensors are not only mounted on one platform. Still, they should also be compatible with software and hardware, e.g. for the same timestamp registration by different sensors. The aim of this article is to propose the synergy between various remote sensing sensors including the ground penetrating radar (GPR), LiDAR (Light Detection and Ranging) sensor and three photogrammetric RGB cameras for damage detection in a pavement in a park alley. The data were acquired with a low-cost platform, in the Pole Mokotowskie Park in Warsaw, Poland. Three drives were made along the same path with the platform, so it was possible to assess the repeatability of the data. Based on the GPR data, orthophotomap, and digital terrain model (DTM) from images, an analysis of the cracks in the pavement was done. The paper proves additive value from the synergy of data collected for the alley also in the form of a common visualization of acquired data. Results presented in the article showed that using mobile mapping platform and technologies describing the situation above and below the ground level enable a more detailed analysis and inspection of the damages in the park alley.

Keywords: damage detection, data integration, data visualization, GPR, LiDAR, non-destructive investigations

[1]PhD., Eng., Warsaw University of Technology, Faculty of Geodesy and Cartography, Pl. Politechniki 1, 00-661 Warsaw, Poland, e-mail: magdalena.pilarska@pw.edu.pl, ORCID: 0000-0001-9494-9863

[2]PhD., Eng., Warsaw University of Technology, Faculty of Geodesy and Cartography, Pl. Politechniki 1, 00-661 Warsaw, Poland, e-mail: krzysztof.bakula@pw.edu.pl, ORCID: 0000-0001-7137-1667

[3]Msc., Eng., Warsaw University of Technology, Faculty of Geodesy and Cartography, Pl. Politechniki 1, 00-661 Warsaw, Poland, e-mail: jakub.gorka@pw.edu.pl, ORCID: 0000-0002-8262-847X

[4]Eng., Warsaw University of Technology, Faculty of Geodesy and Cartography, Pl. Politechniki 1, 00-661 Warsaw, Poland, e-mail: pawel.czernic.stud@pw.edu.pl, ORCID: 0009-0008-6927-5375

[5]PhD., Warsaw University of Technology, Faculty of Civil Engineering, Al. Armii Ludowej 16, 00-637 Warsaw, Poland, e-mail: anna.lejzerowicz@pw.edu.pl, ORCID: 0000-0002-1350-0632

[6]PhD., Eng., Warsaw University of Technology, Faculty of Geodesy and Cartography, Pl. Politechniki 1, 00-661 Warsaw, Poland, e-mail: wojciech.ostrowski@il.pw.edu.pl, ORCID: 0000-0003-2103-1546

[7]PhD., Eng., Lviv Politechnic National University, Institute of Geodesy, 6 Karpinskogo str., Lviv, Ukraine, e-mail: borys.v.chetverikov@lpnu.ua, ORCID: 0000-0001-8677-1735

1. Introduction

In recent years, the importance of monitoring engineering objects using non-invasive methods has increased. Mainly, ground penetrating radar (GPR) has found application in non-invasive analysis of pavement structure [1], as well as roads' and pavements' cracks [2, 3]. One of the main directions of development in this field is the combination of various non-invasive sensors and advanced data analysis, including laser scanning (LiDAR) and GPR [4], that allow for the effect of data synergy providing additional information in the result of the multisensorial data fusion. Data synergy consists of acquiring and combining data from different sensors to achieve better results for problem analysis and research [5]. In GPR and LiDAR sensor integration, in addition to the effect of linking what is above and below the road surface, it may be essential to look for correlations between below and above the ground situation by higher resolution of remote sensing systems from the survey platform (photogrammetry and LiDAR) [6]. LiDAR can also be used to create a digital terrain model (DTM), which allows us to know the surface of the analyzed terrain [7, 8]. This article presents the idea of GPR, LiDAR, and photogrammetry data synergy for detecting damage on roads and pavements. The data used in the article were acquired with a platform equipped with a ground penetrating radar (GPR), Light Detection and Ranging (LiDAR) sensor, and three cameras – one camera mounted in the front of the platform to monitor the pavement and two cameras for surrounding imaging [9].

Road surface monitoring is one of many applications of integrated sensors. Integration of multi-source non-invasive techniques is increasingly being applied to building monitoring and management [10], in monitoring engineering structures such as bridges [11, 12], where autonomous platforms are also proposed [13], roads [14] and in various archaeological research [15, 16]. [17] used visible-spectrum and infrared imagery combined with photogrammetric techniques, terrestrial LiDAR, and microwave to conduct measurements on the historical façades' surfaces and examine the comprehensiveness of the data fusion results [18] performed 3D metric surveys (photogrammetry and laser scanner) and non−invasive geophysical surveys (GPR) to analyze the object's structure and define restoration interventions. According to the Authors, non−destructive testing techniques at different scales have provided assessment tools for building characteristics, state of conservation and building safety.

1.1. GPR and LiDAR data integration

The integration of GPR and LiDAR in the case of pavement analysis is a known approach [19]. The basis for integrating LiDAR data with GPR-acquired data is georeferencing both data types to a single, consistent coordinate system. The GNSS precision positioning technique is the best technique for achieving georeferencing. For even more reliable positioning of both sensors, it is worth using the observations from the IMU, which is part of the LiDAR. Kalman filtering-based algorithms combine the readings from both positioning GNSS and INS units [20].

An essential element in data synergy is precise time synchronization, especially for a LiDAR sensor. It allows for generating a correct point cloud (using readings from the IMU and transforming measured points from the scanner's local system to an external reference system). A key role in this topic is the PPS (Pulse Per Second) signal transmitted by the GNSS receiver. It allows precise timing synchronization with other sensors, which is crucial for accurate measurements [21].

What is more, terrestrial, mobile and Unmanned Aerial Vehicle (UAV) LiDAR data can be integrated with a GPR antenna. For linear objects, mobile LiDAR can be effectively used [22]. For larger areas with irregular locations of GPR measurements, e.g. on archaeological sites, aerial LiDAR can find application [23]. Terrestrial laser scanning (TLS) can be used for smaller areas to accurately measure geometry and detect external defects, as well as in pavements [24].

1.2. GPR and LiDAR data visualization

If both data sources are recorded for the same area, at the same time, the combination of different types of data (GPR – 2D data, and LiDAR – 3D data) into one consistent format allows for obtaining interesting visualisations, which are valuable tools for geospatial analysis [25], as well as in engineering applications [26]. For example, in a road environment, it is possible to accurately detect the technical infrastructure and any changes or defects in the very structure of the analysed section. The main challenge in such visualisation is the adequate representation of elements that are not visible, i.e. data acquired with the GPR unit, in the context of visible data acquired with the LiDAR unit. This is because GPR data is covered by a point cloud derived from laser scanning. Various methods of visualising the combined data are currently being worked on [4]. Among the most popular methods for combining this type of data are:

– exclusion of laser scanning data that obscures underground GPR data,
– lift GPR data above the ground level.

In both cases, it is also worth using different color scales to better distinguish the two types of data [4]. Combining both types of data in a single, consistent form allows to obtain additional and very valuable contextual information, e.g., about the occurrence of sewer manholes, which helps during the analysis to reject artificially created anomalies, for example, by driving a GPR unit over metal utility elements [20].

There are many methods of presenting data and its derivatives acquired from LiDAR and GPR. Among the most popular forms of presentation of laser scanning data are:

– point clouds (full clouds, cross sections, individual point classes),
– digital terrain model (elevation map, hillshade, slope rasters)
– 3D mesh models (both with and without texture),
– 3D solid models.

The most popular forms of GPR data presentation include:

– 2D radargrams,
– depth slice made based on interpolation of 2D radargrams,
– 3D blocks made based on interpolation of 2D radargrams, including georeferenced points from radargrams,
– Solid models – visualizations made using the BIM technique (development of GPR data and other source materials).

Such forms of presentation can be combined freely by selecting the optimal visualisation methods for the issues and the goals to be achieved. Due to the quasi-continuous nature of the data acquired from laser scanning, it is necessary to think carefully about how to display point cloud classes containing points on the ground, which obscure the visualisation of GPR data. Figure 1 is the graph showing the possibilities of how different forms of presentations of those two data sources can be shown in one visualization. The boxes show the necessary processing

of LiDAR and GPR data to achieve more advanced visualization products being the element of data synergy. In the fields separated by a dashed line, the result of data integration is shown.

The most intuitive version is to visualize both raw data sources in a 3D environment. However, this option is not easy, because the data from under the surface is much sparser, and to obtain 3D information about underground objects, it is necessary to transfer from radargrams (cross-sections) to the 3D form in the proper reference system. This variant can include interpretations of images and their results. It would be much easier to visualize ready-made 3D solid models created from the data, but it is quite an expensive product that requires a lot of money (Fig. 1).
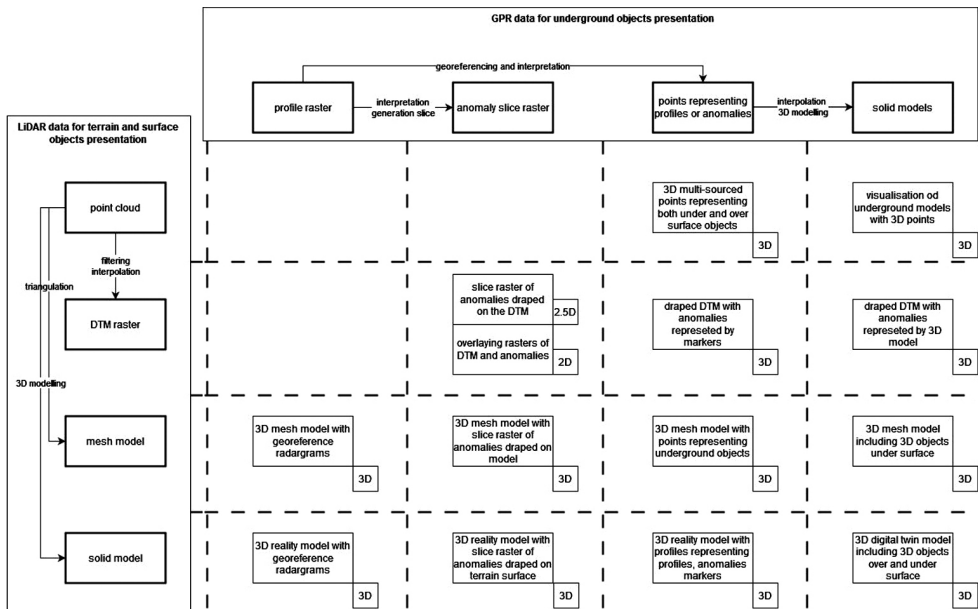
Fig. 1. Opportunities for synergy of GPR and LiDAR

A more accessible 3D model option is the mesh model. In this case, the underground objects must be properly modelled with solids. A simpler option is to visualize the GPR observation rasters against the background of a point cloud – 2.5D approach. This approach does not reveal the true depth of the anomaly measured by the GPR, but it does orient the GPR data in terms of where it was obtained. The depth can be estimated from the interpretation of the oriented raster. Unfortunately, the basic option for data visualization is still the 2D presentation. It can be either work on cross-sections or DTM visualization with the GPR observation raster superimposed. Sometimes they are modified by the orientation of the cross-section in space.

The aim of this article is to propose an investigation and visualization approach based on the remote sensing sensors synergy. On the mapping platform GPR, LiDAR and photogrammetric cameras were integrated, together with the GNSS antenna for position measurement, thus all the acquired data had their location in one selected coordinate system. Such a wide data integration which includes both software and hardware integration is a novel approach in the field of pavement monitoring and damage detection.

2. Methodology

2.1. Investigation site

The measurement area was located in the eastern part of Pole Mokotowskie, bounded by Waryńskiego, Batorego, Al. Niepodległości and Al. Armii Ludowej streets (Fig. 2). According to the local spatial development plan, Pole Mokotowskie is a complex of park areas, organised greenery, and accompanying sports and service facilities. In the 1990s, work was carried out on the construction the Politechnika subway station, the range of which included a part of Pole Mokotowskie, where the measurements with the platform were performed. Most of the existing park paths were also built in the 1990s. There are park paths of various constructions: asphalt, paving slabs, granite blocks, cobblestones, gravel, and dirt. The analysed part is located on a park path with an asphalt surface. The test area is presented on the Fig. 2. The map was prepared in ETRF2000-PL / CS92 coordinate system (EPSG 2180).

Fig. 2. Test area in Pole Mokotowskie, Warsaw where the measurements were performed (trajectory of measurement showed in green, left side) and platform presentation (right side)

Based on the regulations in effect in the 1990s for designing various pathways, it can be assumed that the surveyed pavement is most likely constructed of two layers: a 4 cm thick asphalt concrete wearing course and a 10 cm thick aggregate substructure.

2.2. Acquired data

The mobile mapping platform used for the data acquisition is equipped with multiple sensors [27], which are:
– Livox Avia LiDAR used for the acquisition of point clouds and navigation using SLAM technology,
– Trimble R9S GNSS receiver for global reference system positioning,
– Two Sony A6000 cameras for surrounding imaging,
– Sony A7R camera to acquire surface data in front of the platform,
– Cobra CBD GPR (ground penetrating radar) to subsurface data acquisition.

2.2.1. Data integration

Data integration within the platform was divided into two main parts: real-time integration, providing data acquisition with a consistent timeline, and data postprocessing. The former objective was achieved by establishing communication between sensors and a processing unit used as a time server. In postprocessing, sensor data is refined using other sensors' time and location information, transforming all sources into a uniform and consistent spatial reference system.

2.2.2. GPR data

Ground penetrating radar data was obtained with Cobra CBD WiFi GPR (Radarteam Sweden AB), a 2-channel GPR antenna, a triple frequency unit with nominal frequencies 200, 400, and 800 MHz and an operating bandwidth of 50–1400 MHz. This type of GPR unit can be used for both shallow and deep targets as the pulse from the transmitting antenna first enters 800 MHz, then 400 MHz, and finally 200 MHz. In this way, a blended or mixed pulse is generated from these 3 antennas, and it is transmitted into the investigated medium [28]. Data was acquired using a control unit – a tablet with installed Prism2 software. Penetration depth was up to 5 meters.

2.2.3. Photogrammetric data

The images were acquired with 3 cameras mounted on the platform. Two of them – Sony A6000 cameras – were used to map the surroundings of the pavement. A Sony A7R camera was mounted on the front of the platform and was used to take images of the pavement in front of it.

2.2.4. Livox Avia

LiDAR data was delivered by Livox Avia, a lightweight, compact sensor that registers data with a frequency 240 000 points per second. The maximum number of registered echoes for one laser beam is 3. Additionally, this sensor has two modes of scanning: non-repetitive (circular scanning) and repetitive (line scanning). It is a lightweight, budget, and compact LiDAR unit that can be used, e.g., on unmanned aerial vehicles (UAV) and mobile platforms like the one presented in this article.

2.3. Data preparation

The images were processed using Agisoft Metashape software. Thanks to the GNSS receiver, the images had external orientation parameters, i.e., information about the location where an image was acquired. Ground control points (GCPs) were used for image orientation. The GCPs were marked on the pavement as white crosses. From the images, a dense point cloud, DTM, and orthomosaic were generated.

LiDAR data was processed using numerous programs and programming libraries. Among the software, the most important relevant is ROS (robotic operation system) core, a program that oversees the execution and communication between various ROS "nodes". Packages "Livox SDK" and "Livox ROS driver" enable the handling of LiDAR data packets from this specific LiDAR unit, and FAST_LIO library [29].

The GPR data were processed using the dedicated software Prism2 (Radarteam Sweden AB). Basic data processing was performed, including zero-level correction, automatic gain control, and background removal. After data processing, based on trace curve, point info, and hyperbola fitting, potential places of occurrence of roots in the studied area were determined and marked on radargrams (Fig. 3). The GPR data processed this way was exported to a point cloud in text format, including the 3D position and the value of the recorded wave amplitude. Using the author's script, the trajectories of individual GPR passes used in subsequent analyses were extracted from such prepared point clouds.
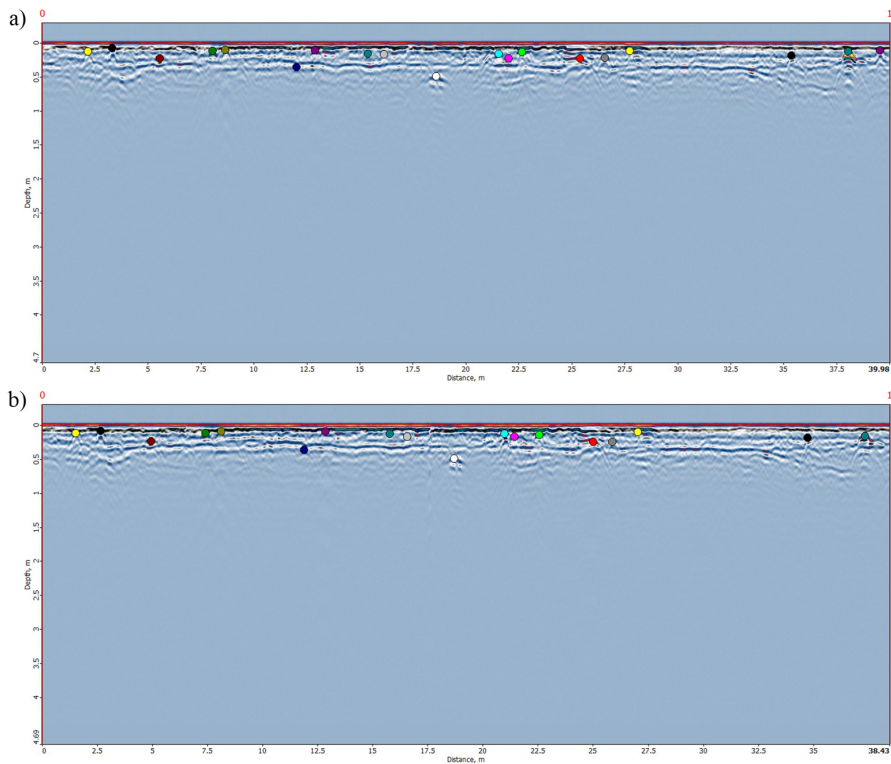
Fig. 3. GPR data example: radargrams (obtained with multifrequency Cobra CBD GPR, with penetration time of 100 ns) from two drives with marked anomalies (tree roots) using a different color for corresponding anomalies; (a) GPR profile no. 3, drive no. 1, (b) GPR profile no. 3, drive no. 2

2.4. Methodology of data interpretation

The data was visually analysed to analyse the damage to the pavement. From photogrammetric data, a dense point cloud was generated. Cross sections were visualised based on the point cloud, and a DTM was produced. Based on the DTM, a more detailed investigation was conducted based on different products created from the DTM, e.g., a hillshade model.

3. Results

3.1. Image processing

Images were oriented and processed using Agisoft Metashape software. For image orientation GCPs marked as white crosses were marked on the pavement. Images from each camera were oriented separately. The images were oriented with subcentimeter accuracy (2–4 mm, depending on the drive). After image orientation, a dense point cloud was built, and DTM was generated. From Sony A7R images, an orthophotomap was also created.

3.2. Data analysis and results

Firstly, the potential of side-looking cameras was analysed in surface modelling. Regarding the Sony A6000 results, the DTM was insufficient for the analysis of the cracks in the pavement (Fig. 4). The DTM was smoothed, and a less detailed model was compared to the DTM from the Sony A7R. As expected, these cameras on the platform can be used mainly for surrounding mapping.
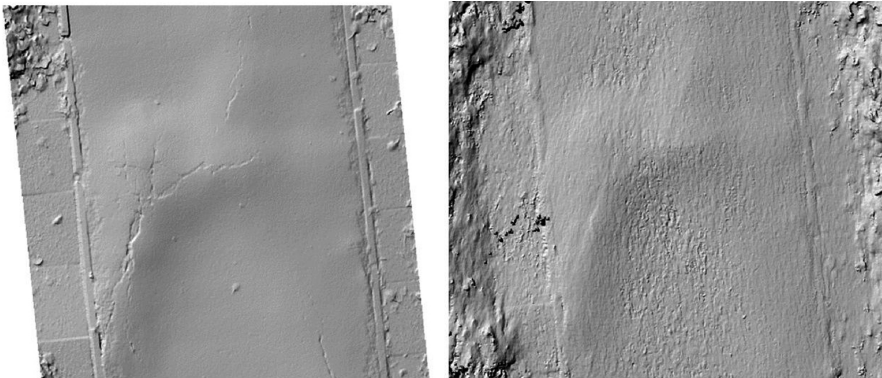
Fig. 4. Comparison of DTMs generated from Sony A7R camera (left) and Sony A6000 camera (right)

The Sony A7R camera was tilted 40 degrees from the zenith level and was dedicated to pavement imaging. Thus, as expected, the DTM was more detailed and less smooth compared to the DTM from the Sony A6000 camera (Fig. 4). Thus, in further analysis, only the DTM from the Sony A7R camera is taken into account.

During the first data processing, two DTMs with different resolutions were generated: 0.5 mm and 5 mm to decide what is the best resolution of the model. The high difference between the DTMs was calculated by subtracting 5 mm DTM from 0.5 mm DTM. As a result, a differential DTM (dDTM) was calculated. Referring to Fig. 5, the difference between the DTMs is not high. On a flat area, the difference was close to 0, while on some crack-type changes, it is about 1 mm. Moreover, 5 mm DTM is smoother than 0.5 mm DTM, but on 0.5 mm DTM, the same cracks were visible as on 5 mm DTM. Therefore, a 5 mm DTM is used to further analyse the article.
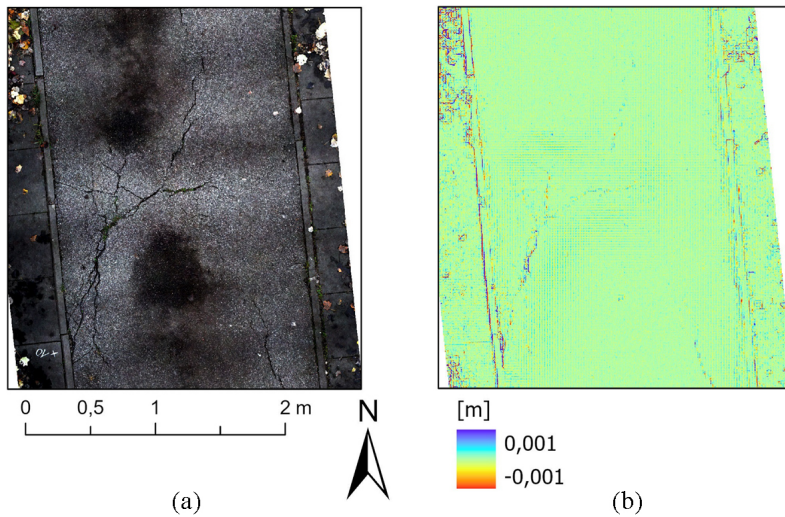
Fig. 5. Ortophoto of pavement fragment (a) and dDTM calculated for 5mm and 0.5 mm DTMs fromSony A7R camera (b)

During the measurement, 3 drives (with 4 strips) were conducted to map and collect the data for the pavement. Data from three drives were then processed. Thanks to that, the repeatability of the data could be checked. The images were oriented using GCPs. Next, DTMs were generated for the 3 drives, and the RMS value was calculated based on the mean value to determine the accuracy of the DTM referring to the average value of elevation. In Fig. 6, the RMS values are presented. For most of the area accuracy of less than 1 mm was obtained, which is sufficient for this type of analysis and proves the coherence of all measurements during image orientation from all three drives. The map was prepared in ETRF2000-PL / CS92 coordinate system (EPSG 2180).
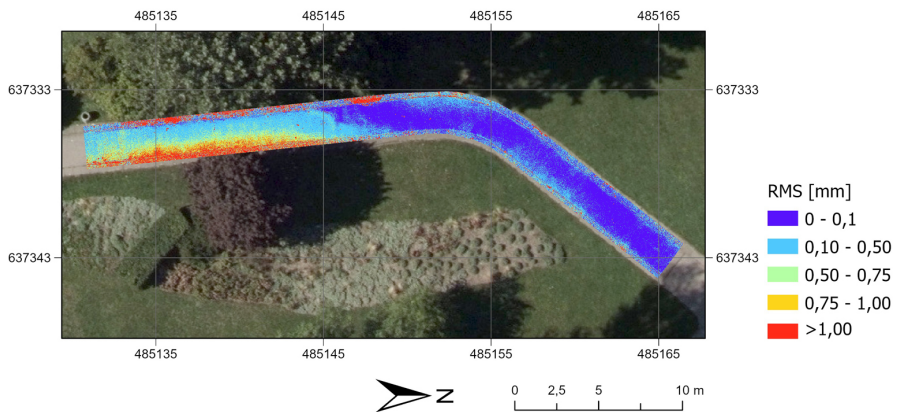
Fig. 6. RMS value calculated based on the mean value for the DTMs generated from 3 datasets

For DTM analysis, a hillshade model in ArcGIS Pro was generated. DTM hillshade model was compared with an orthophotomap to check whether there are some cracks or other elements that are visible on one of them and not visible on the second one. It can be found that some damages were visible on the orthophotomap but not visible on the hillshade DTM (Fig. 7). This might be a crack that is very tiny or does not characterise a height change that can be observed on the DTM of this accuracy.
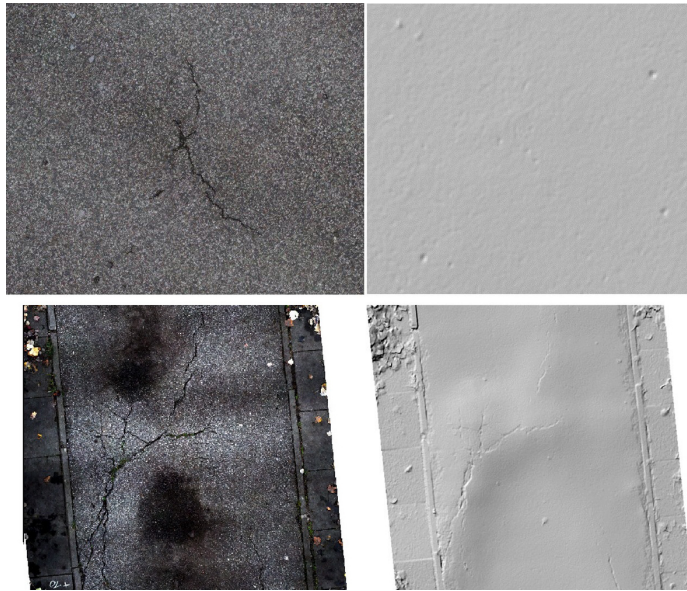
Fig. 7. Examples of cracks visible on the orthophotomap but not visible on the DTM (above) and visible on both orthophotomap and the DTM (below)

3.3. Lidar and photogrammetric data comparison

From the Livox laser scanner, a point cloud was also delivered, which was georeferenced based on the trajectory registered by the GNSS receiver and SLAM algorithm. The laser scanner registered the points both in the alley and the surroundings; thus, trees and other elements near the alley were visible in the point cloud. Only the part of the point cloud which covers the alley is analysed in the article.

The Livox Avia sensor data were analysed for data accuracy and compared to the point cloud generated from the Sony A7R images. Both point clouds were visualised, and cross-sections were drawn (Fig. 8). Analysing them, it can be seen that the point cloud from images is more consistent, i.e. the point distribution is less noisy, and it would be easier to assess where the actual pavement is located based on this dataset. Livox point cloud is much noisier; thus, Livox sensor can be used for location and navigational purposes rather than for surface measurement and analysis. The noise in photogrammetric point cloud was milimeter-level and in the case of a low-cost LiDAR unit, it was about 5 centimetres.
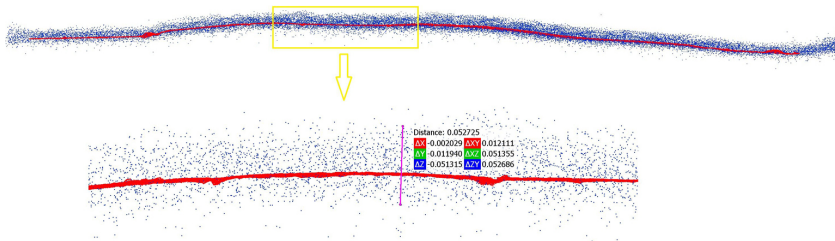
Fig. 8. A cross-section through Sony A7R (red points) and Livox (blue) point clouds

From the point cloud, a DTM was generated. In Fig. 9 a comparison of DTM hillshades from Sony A7R images and Livox point cloud are presented. This figure shows the differences between the data quality from the Sony images and Livox data. The Sony A7R DTM is smooth, and the small hills and cracks can be noticed. Regarding the Livox DTM, for the lowest presented resolution, which is 1 cm, the DTM is noisy because of the point cloud quality. Lower-resolution DTMs are smoother, and the hill is more clearly visible. What is essential is that the cracks on the hill are not visible on the hillshade DTM. Considering all shown analyses, due to insufficient data quality of LiDAR data, it was decided that this sensor was used only for navigational purposes providing information about the trajectory of the platform in integration with the GNSS antenna.
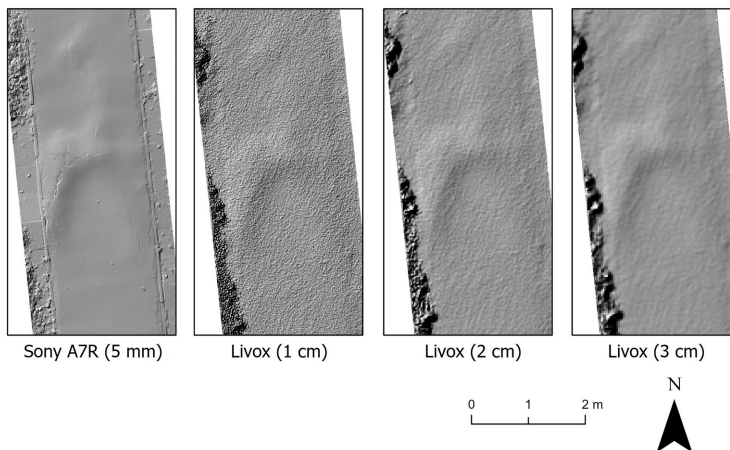
Fig. 9. Comparison of DTM hillshades from Sony A7R images and Livox point cloud

3.4. Marker measurements on radargrams and their repetitiveness

The locations of GPR anomalies were determined on all GPR profiles. They were exported in Prism2 software into text form containing, among other things, the trace number and depth. On this basis, it was combined with the previously exported trajectories of the crossings. The final

result was the acquisition of accurate horizontal and depth-determined markers delineating GPR anomalies. The repeatability of the markers' measurement was examined to assess accuracy capabilities. Differences in markers' locations and depth were presented in Table 1.

Table 1. Repeatability of marker measurements of radargrams from two drives

	d_x	d_y	d_xy	d_depth
Mean [m]	0.018	−0.010	0.020	0.002
Median [m]	0.013	−0.005	0.014	0.010
Standard deviation STD [m]	0.082	0.078	0.113	0.030

Analyzing the results presented in Table 1, the standard deviation of the markers' location repetitiveness (d_xy) is about 8 cm. The trajectory registration influenced the final accuracy. In the park alley, trees, buildings, and other elements affect the GNSS measurement. Thus, the accuracy of the registered trajectory can be different depending on the part of the area. Additionally, the speed of the drives can affect the location accuracy of the markers (kinematic measurements) and the human factor, i.e. markers' identification. Differences between measurements of the depth detected in underground objects were repeated with a standard deviation of 3 cm.

3.5. Final visualization integrated data

Using the collected data from the mobile platform, a 3D visualization for two selected data sources is proposed. In Fig. 10 the 3D views of data synergy including a 3D point cloud from LiDAR (representing the surroundings), a GPR radargram presented as georeferenced points, and interpreted markers (red lines) presenting the anomalies' location and their depth. Georeferencing of final data sources in a homogeneous three-dimensional environment is a solution that provides more information that cans be verified and compared using various techniques. They can be complementary to each other.
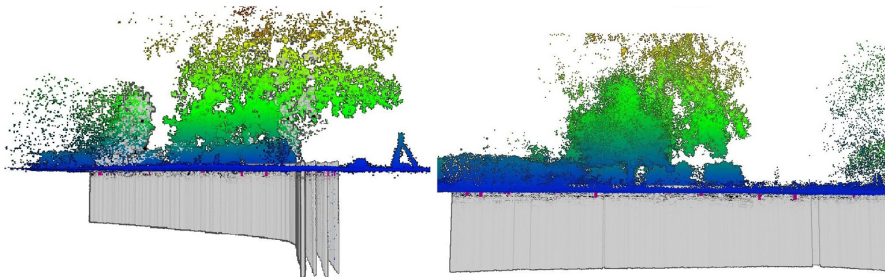
Fig. 10. Example of the visualization including LiDAR and GPR data (red lines: markers – GPR anomalies)

4. Discussion

Laser scanning data (terrestrial/mobile) fusion together with GPR data was proved to be useful in many applications, from bridge condition assessment [11, 12], up to archaeology [15]. Similar results to those presented in this article can be found in the literature. In [25], the Authors also acquired laser scanning data and GPR data using the mobile platform to prepare a common visualization of them. According to the authors, if there is damage in the road, such visualization can be used to quickly and accurately determine the state of the pavement above and below it. Within this article a common visualization of acquired data was also proposed (Fig. 10). Similar conclusions were drawn by [22], where the authors suggested that the analysis of the pavement deformations using mobile laser scanning together with GPR allows the evaluation of whether the surface deformation involves deeper layers or only the surface. Comparable data fusion was done by [26], where a 3D model was integrated with radargrams instead of the point cloud. In the case of a low-cost LiDAR unit used in this article, the results for road/alley modelling are still not sufficient and this sensor was used only for navigational purposes with the SLAM algorithm. The technology that can bring 3D point clouds with appropriate quality, both accuracy and density, is dense image matching using photogrammetric images taken with a digital camera. The approach and mobile platform presented in this article proved, that such data synergy can be successfully applied in pavement inventory for damage detection, as well as in other applications, e.g. in archaeology for inventory of the objects below the ground, especially relics of objects in the ground.

5. Conclusions

The article introduced the synergy of remote sensing data collected with a low-cost mobile mapping platform for detecting and predicting damages. Data acquired from mobile platforms can be complementary in case of pavement investigation. From the images, a DTM and an orthophotomap were generated. Together with markers measured on the radargrams, a 2D analysis was conducted. Orthophotomap and DTM, together with the markers, answered questions about whether the anomalies found underground have effects on the ground, e.g. as cracks, or if the impact of anomalies found underground will be visible in the future. Additionally, a point cloud from LiDAR, generated from the images, and a point cloud from GPR or a radargram provide a 3D presentation of obtained results. GPR and 3D point cloud data fusion can find applications in many fields. This article also integrated the data with a high-resolution orthophotomap and point cloud processing to the elevation model generated from a Sony A7R camera. Such fusion brings the synergy effect when the end-user can notice the additive value of such integration by comparing or completing the results of observation.

The limitation of proposed approach is the time that is necessary to acquire and process the data. Additionally, because of changing environment (e.g. trees), there were places with weak GNSS signal. In further research the Authors will work on enhancement of the trajectory accuracy so that there will not be a need to make an advanced data processing and adjustment. Additionally, there are GPRs that can be mounted on the UAVs. Acquiring and integration

of the GPR data and images from the UAV could be faster and thus more efficient. In more advanced studies on the road/pavement/construction damages there are other approaches that can be used in the future, including geological [30] and archeological investigations [31].

Funding

References

[1] M. Varela-González, M. Solla, J. Martínez-Sánchez, and P. Arias, "A semi-automatic processing and visualisation tool for ground-penetrating radar pavement thickness data", *Automation in Construction*, vol. 45, pp. 42–49, 2014, doi: 10.1016/J.AUTCON.2014.05.004.

[2] M.E. Torbaghan, W. Li, N. Metje, M. Burrow, D.N. Chapman, and C.D.F. Rogers, "Automated detection of road cracks using ground penetrating radar", *Journal of Applied Geophysics*, vol. 179, art. no. 104118, 2020, doi: 10.1016/j.jappgeo.2020.104118.

[3] L. Krysiński and J. Sudyka, "GPR abilities in the investigation of the pavement transversal cracks", *Journal of Applied Geophysics*, vol. 97, pp. 27–36, 2013, doi: 10.1016/J.JAPPGEO.2013.03.010.

[4] D. Merkle, C. Frey, and A. Reiterer, "Fusion of ground penetrating radar and laser scanning for infrastructure mapping", *Journal of Applied Geodesy*, vol. 15, no. 1, pp. 31–45, 2021, doi: 10.1515/jag-2020-0004.

[5] B. Chetverikov, "Application of radar interferometry and ground-penetrating radar imaging for monitoring historical and cultural lands", *Modern Achievements in Geodetic Science and Industry*, vol. 45, no. 1, pp. 153–160, 2023.

[6] A.T. Hassan and D. Fritsch, "Integration of laser scanning and photogrammetry in 3D/4D cultural heritage preservation – A Review", *International Journal of Applied Science and Technology*, vol. 9, no. 4, p. 76–91, 2019, doi: 10.30845/ijastv9n4p9.

[7] A. Plichta and A. Piasecki, "Lidar and ground penetrating radar data in determining road surface conditions and geological characteristics of unstable soils", *Technical Sciences/University of Warmia and Mazury in Olsztyn*, vol. 20, no. 2, pp. 111–129, 2017.

[8] I. Rodríguez-Santalla, D. Gomez-Ortiz, T. Martín-Crespo, et al., "Study and Evolution of the Dune Field of La Banya Spit in Ebro Delta (Spain) Using LiDAR Data and GPR", *Remote Sensing*, vol. 13, no. 4, 2021, doi: 10.3390/rs13040802.

[9] R. Filzwieser, V. Ivanišević, G. J. Verhoeven, et al., "Integrating geophysical and photographic data to visualize the quarried structures of the Roman town of Bassianae", *Remote Sensing*, vol. 13, no. 12, art. no. 2384, 2021, doi: 10.3390/rs13122384.

[10] Y. El Masri and T. Rakha, "A scoping review of non-destructive testing (NDT) techniques in building performance diagnostic inspections", *Construction and Building Materials*, vol. 265, art. no. 120542, 2020, doi: 10.1016/j.conbuildmat.2020.120542.

[11] S. Cafiso, A. Di Graziano, D. Goulias, M. Mangiameli, and G. Mussumeci, "Bridge monitoring combining laser scanning and ground penetrating radar", *AIP Conference Proceedings*, vol. 2116, no. 1, 2019, doi: 10.1063/1.5114287.

[12] S. Cafiso, A. Di Graziano, D. Goulias, M. Mangiameli, and G. Mussumeci, "Implementation of GPR and TLS data for the assessment of the bridge slab geometry and reinforcement", *Archives of Civil Engineering*, vol. 66, no. 1, pp. 297–308, 2020, doi: 10.24425/ace.2020.131789.

[13] D. Merkle, A. Schmitt, and A. Reiterer, "Concept of an autonomous mobile robotic system for bridge inspection", in *Remote Sensing Technologies and Applications in Urban Environments V*. SPIE, 2020, pp. 34–49, doi: 10.1117/12.2570633.

[14] W. Li, M. Burrow, N. Metje, and G. Ghataora, "Automatic road survey by using vehicle mounted laser for road asset management", *IEEE Access*, vol. 8, pp. 94643–94653, 2020, doi: 10.1109/access.2020.2994470.

[15] N. Kamp, S. Russ, O. Sass, G. Tiefengraber, and S. Tiefengraber, "A Fusion of GPR-and LiDAR-Data for Surveying and Visualisation of Archaeological Structures-a case example of an archaeological site in Strettweg, District of Murtal, Austria", in *EGU General Assembly Conference Abstracts*. 2014.

[16] I. Puente, M. Solla, S. Lagüela, and J. Sanjurjo-Pinto, "Reconstructing the Roman Site 'Aquis Querquennis' (Bande, Spain) from GPR, T-LiDAR and IRT Data Fusion", *Remote Sensing*, vol. 10, no. 3, art. no. 379, 2018, doi: 10.3390/rs10030379.

[17] E. Adamopoulos, C. Colombero, C. Comina, et al., "Integrating multiband photogrammetry, scanning, and GPR for built heritage surveys: the façades of Castello del Valentino", *ISPRS Annals of the Photogrammetry, Remote Sensing and Spatial Information Sciences*, vol. 8, pp. 1–8, 2021, doi: 10.5194/isprs-annals-VIII-M-1-2021-1-2021.

[18] M. Cozzolino, A. Di Meo, and V. Gentile, "The contribution of indirect topographic surveys (photogrammetry and laser scanner) and GPR investigations in the study of the vulnerability of the Abbey of Santa Maria a Mare, Tremiti Islands (Italy)", *Annals of Geophysics*, vol. 62, no. 3, 2019, doi: 10.4401/ag-7987.

[19] A. Elseicy, A. Alonso-Diaz, M. Solla, M. Rasol, and S. Santos-Assunçao, "Combined use of GPR and other NDTs for road pavement assessment: An overview", *Remote Sensing*, vol. 14, no. 17, art. no. 4336, 2022, doi: 10.3390/rs14174336.

[20] J. Wolf, S. Discher, L. Masopust, S. Schulz, R. Richter, and J. Döllner, "Combined visual exploration of 2d ground radar and 3d point cloud data for road environments", *The International Archives of the Photogrammetry, Remote Sensing and Spatial Information Sciences*, vol. 42, pp. 231–236, 2018, doi: 10.5194/isprs-archives-XLII-4-W10-231-2018.

[21] X. Niu, K. Yan, T. Zhang, Q. Zhang, H. Zhang, and J. Liu, "Quality evaluation of the pulse per second (PPS) signals from commercial GNSS receivers", *GPS Solutions*, vol. 19, pp. 141–150, 2015, doi: 10.1007/s10291-014-0375-7.

[22] L.B. Ciampoli, A. Calvi, A. Di Benedetto, M. Fiani, and V. Gagliardi, "Ground Penetrating Radar (GPR) and Mobile Laser Scanner (MLS) technologies for non-destructive analysis of transport infrastructures", in *Earth Resources and Environmental Remote Sensing/GIS Applications XII*. SPIE, 2021, pp. 166–174, doi: 10.1117/12.2599283.

[23] R. Di Maio, A. Emolo, A. Frisetti, et al., "Reconstruction of archaeological contexts through the integrated use of airborne LiDAR and geophysical survey: The case study of San Pietro Infine (Caserta, southern Italy)", *Journal of Archaeological Science: Reports*, vol. 49, art. no. 104013, 2023, doi: 10.1016/j.jasrep.2023.104013.

[24] S. Lagüela, M. Solla, I. Puente, and F.J. Prego, "Joint use of GPR, IRT and TLS techniques for the integral damage detection in paving", *Construction and Building Materials*, vol. 174, pp. 749–760, 2018, doi: 10.1016/j.conbuildmat.2018.04.159.

[25] Y. Zhou, Q. Hu, J. Zhang, P. Zhao, F. Yu, and M. Ai, "An Ground and Under-Ground Urban Roads Surveying Approach Using Integrated 3d LIDAR and 3D GPR Technology", *ISPRS Annals of the Photogrammetry, Remote Sensing and Spatial Information Sciences*, vol. 10, pp. 101–107, 2022, doi: 10.5194/isprs-annals-X-3-W2-2022-101-2022.

[26] T. Bicudo and I. Nakakura, "3D Models Integrating GPR and Apple LiDAR to Improve Results Visualization in Engineering and Geotechnical Applications", in *NSG2023 3rd Conference on Geophysics for Infrastructure Planning, Monitoring and BIM*. 2023, pp. 1–5, doi: 10.3997/2214-4609.202320080.

[27] K. Bakuła, A. Lejzerowicz, M. Pilarska-Mazurek, et al., "Sensor integration and application of low-sized mobile mapping platform equipped with lidar, GPR and photogrammetric sensors", *The International Archives of the Photogrammetry, Remote Sensing and Spatial Information Sciences*, vol. 43, p. 2022, doi: 10.5194/isprs-archives-xliii-b1-2022-167-2022.

[28] RadarTeam, "RadarTeam, Sweden".

[29] W. Xu, Wei, and F. Zhang, "Fast-lio: A fast, robust lidar-inertial odometry package by tightly-coupled iterated kalman filter", *IEEE Robotics and Automation Letters*, vol. 6, no. 2, pp. 3317–3324, 2021, doi: 10.1109/LRA.2021.3064227.

[30] M. Maślakowski, A. Lejzerowicz, G. Pacanowski, and R. Kuszyk, "The use of non-invasive ERT method to diagnose karst in road engineering in the Lublin Upland (Poland)", *Archives of Civil Engineering*, vol. 70, no. 1, pp. 557–571, 2024, doi: 10.24425/ace.2024.148928.

[31] T. Godlewski, R. Mieszkowski, and M. Maślakowski, "From legend to discovery – historical and geotechnical conditions related to the discovery of tunnels under The Castle Hill in Szczecin", *Archives of Civil Engineering*, vol. 69, no. 1, pp. 453–467, 2023, doi: 10.24425/ace.2023.144183.

Synergia danych teledetekcyjnych pozyskanych z wykorzystaniem niskobudżetowej mobilnej platformy kartującej do wykrywania i predykcji uszkodzeń na przykładzie alei w parku

Streszczenie:

Synergia danych obejmuje pozyskiwanie i łączenie danych z różnych sensorów w celu wykonania lepszej jakości analiz i uzyskania lepszych wyników badań. W celu zapewnienia bardziej kompleksowej analizy danych, oprócz tego, że sensory są montowane na jednej platformie, powinny być one również kompatybilne z oprogramowaniem i sprzętem, np. w celu rejestracji tego samego znacznika czasu przez różne sensory. Celem tego artykułu jest zaproponowanie synergii między różnymi sensorami teledetekcyjnymi, w georadarem (GPR), czujnikiem LiDAR (Light Detection and Ranging) i trzema fotogrametrycznymi kamerami RGB do wykrywania uszkodzeń chodnika w alejce parkowej. Dane zostały pozyskane za pomocą niskokosztowej platformy w parku Pole Mokotowskie w Warszawie. Wykonano trzy przejazdy platformą po tej samej trasie, dzięki czemu możliwa była ocena powtarzalności danych. Na podstawie danych z georadaru, i numerycznego modelu terenu (NMT) ze zdjęć przeprowadzono analizę pęknięć w nawierzchni. W artykule udowodniono wartość dodaną wynikającą z synergii również w postaci wspólnej wizualizacji pozyskanych dla chodnika danych. Wyniki przedstawione w artykule wykazały, że wykorzystanie mobilnej platformy oraz technologii opisujących sytuację nad i pod poziomem gruntu umożliwia bardziej szczegółową analizę i inspekcję uszkodzeń w alejce parkowej.